PHOTONIC SENSORS / Vol. 9, No. 3, 2019: 284–292

Performance Analysis of Silicon and Blue Phosphorene/MoS_2 Hetero-Structure Based SPR Sensor

Akash SRIVASTAVA and Y. K. PRAJAPATI*

Department of Electronics and Communication Engineering, Motilal Nehru National Institute of Technology Allahabad, Allahabad 211004, Uttar Pradesh, India

*Corresponding author: Y. K. PRAJAPATI E-mail: yogendrapra@mnnit.ac.in and yogendrapra@gmail.com

Abstract: Surface plasmon resonance (SPR) sensor based on the blue phosphorene/MoS_2 hetero-structure is presented to enhance the performance parameters, i.e., sensitivity, detection accuracy, and quality factor. The blue phosphorene/MoS_2 hetero-structure works as an interacting layer with the analyte for the enhancement of the sensitivity of the sensor. It is observed that the sensitivity of blue phosphorene/MoS_2 based sensor (i.e., structure-II) is improved by 5.75%, from the conventional sensor (i.e., structure-III). Further, an additional silicon nanolayer is introduced between the metal layer and blue phosphorene/MoS_2 hetero-structure. The sensitivity of the proposed blue phosphorene/MoS_2 hetero-structure with a silicon layer SPR sensor, i.e., structure-I, is enhanced by 44.76% from structure-II and 55.75% from structure-III due to an enhancement in the evanescent field near the metal-analyte interface. Finally, it is observed that at the optimum thickness of silicon between the gold layer and blue phosphorene/MoS_2, performance parameters of the sensor are enhanced.

Keywords: Surface plasmon; blue phosphorene; MoS_2; sensitivity

Citation: Akash SRIVASTAVA and Y. K. PRAJAPATI, "Performance Analysis of Silicon and Blue Phosphorene/MoS_2 Hetero-Structure Based SPR Sensor," *Photonic Sensors*, 2019, 9(3): 284–292.

1 Introduction

Surface plasmon resonance (SPR) sensors have garnered attention owing to their unbeatable properties like high sensitivity, fast response, real-time detection, ability to detect a very minute change in sensing layer refractive index, and label-free detection [1, 2]. These properties make them useful in the area of medical, health, biosensing application, drug analysis, etc. [3, 4]. The basic idea of SPR sensors is based on surface plasmons (SPs). SPs are collective oscillating electrons or electromagnetic waves that are confined to the thin layer of metals like gold (Au), silver (Ag), and aluminum (Al), etc. [1]. They are also called as surface plasmon polaritons (SPP) or surface plasmons waves (SPW) [2]. To obtain the SPR condition, the wave vector of incident light must match the wave vector of an SPW, and the reflectance dip is observed at SPR condition in the reflectance curve due to attenuated total reflection (ATR). The sensing performance of the SPR sensor can be obtained from the reflectance curve. The attachment of analyte or binding of biomolecules on the sensor surface is one of the important parts of the sensor for accurate and better performance. In that regard, graphene has been used as a bio-recognition element (BRE) because it increases

Received: 7 August 2018 / Revised: 30 November 2018

DOI: 10.1007/s13320-019-0533-1
Article type: Regular

the adsorption on the sensor surface [5, 6]. It has been observed that the adsorption of carbon-based molecules of the analyte with π-bond of graphene increases the enhancement of the performance of the SPR sensor. Also, other two-dimensional (2D) materials such as MoS_2, WS_2, WSe_2, black phosphorus, and blue phosphorene (blue P) have been noted for sensitivity enhancement [7–10]. 2D materials with the graphene-based hetero-structure have been reported for the SPR sensor [11, 12]. It is seen that hetero-structure based sensors provide a better sensitivity compared with that of individual graphene or 2D materials-based sensors [13]. Phosphorene material has been reported for sensing application [14, 15]. Recently, a hetero-structure of the blue P with MoS_2 monolayer is utilized to enhance the sensitivity due to both materials possess hexagonal lattice structures [13, 16]. Due to hexagonal lattice structures of both, blue P is easily stacked on the top of MoS_2 and forms a hetero-structure with the help of Van der Waals forces of attraction [15, 16]. It is worth noting that the lattice parameter of the blue P matches with MoS_2 perfectly. In addition, the blue P can especially adsorb the oxygen gas (O_2) on its surface [15]. Hence, the presented phosphorene/MoS_2 hetero-structure can detect O_2 gas. In addition, the presented structure can detect various viruses after having suitable linker. Recently, a thin layer of silicon (Si) over plasmonic metal has been used to improve the sensitivity of the SPR sensor since it increases the field intensity of the excitation light at the silicon–sensing layer interface [6, 10]. The field intensity at dielectric interfaces increases because of the high absorption behavior of the metal and silicon layer. It, as a result, enhances the excitation of SPs [17, 18]. The objective of the present work is to explore the sensing capabilities of blue P/MoS_2 hetero-structure in the SPR sensor. Further, the Si layer is incorporated between the blue P/MoS_2 hetero-structure and gold for sensitivity enhancement in the proposed work. The paper is ordered as follows: Section 2 contains the requisite theoretical and mathematical background of the proposed sensor. Section 3 contains discussion on the comparative study of the obtained results. Section 4 focuses on the conclusions.

2. Design consideration and theoretical background

2.1 Design consideration of proposed SPR sensor

The schematic diagram of a proposed SPR sensor configuration is given in Fig. 1. The operating wavelength (λ) of the incident p-polarized light source is considered as 632.8 nm.

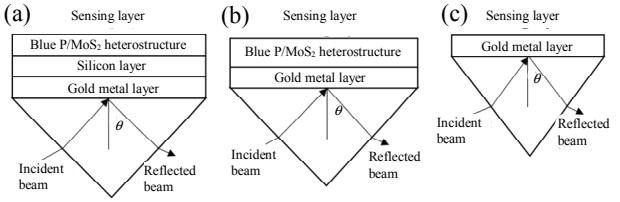

Fig. 1 Schematic diagram of a proposed SPR sensor configuration: (a) blue P/MoS_2 hetero-structure with the silicon layer SPR sensor, i.e., structure-I, (b) blue P/MoS_2 hetero-structure based SPR sensor, i.e., structure-II, and (c) conventional SPR sensor, i.e., structure-III.

The first layer of the sensor is a light coupling glass prism (BK7) with the refractive index (RI) 1.5151 [6], and a gold (Au) layer having a thickness of 50 nm and RI of 0.1726 + i 3.4218 [6, 9] is attached on the top of a glass prism. In the proposed sensor, the thickness of the Au layer is selected to obtain the minimum possible value of reflectance because this optimization tends to strengthen the evanescent field. An additional silicon nanolayer (i.e., the third layer) having RI 3.916 [10] is used between the metal layer and blue P/MoS_2 to enhance the evanescent field near the metal-dielectric material interface in order to increase the stability and sensitivity of the sensor [18]. The thickness of the silicon layer is 2 nm. As a fourth layer, a blue P/MoS_2 hetero-structure is applied, which is in direct contact with the sensing layer. The RI of blue P/MoS_2 is 2.7915+i 0.335, and the thickness of the hetero-structure monolayer is fixed at 0.75 nm [16]. The last layer of this sensor i.e., the fifth-layer is the

sensing layer. The refractive index of the sensing layer is varied between RI of pure water i.e., before absorption of biomolecules (1.33) and that of impure water i.e., after absorption of biomolecules (1.36). Finally, three structures of the SPR sensor are made by using above defined five layers as shown in Table 1.

Table 1 Schematic structure of the SPR sensor.

Structure	Layer arrangement
I	Prism/gold/silicon layer/blue P/MoS_2 hetero-structure/ sensing layer
II	Prism/gold/blue P-MoS_2 hetero-structure/sensing layer
III	Prism/gold layer/sensing layer

It is worth noting here that the evanescent field of the surface plasmon wave is highly sensitive towards any change in thickness, refractive index, and extinction coefficient. Any change in these parameters disturbs the wave vector matching condition of the incident light and surface plasmon wave which is achieved at a particular angle of incidence beyond critical angle $[\theta_c = \sin^{-1}(n_s / n_p)]$, where n_s and n_p are refractive indices of the sensing medium and prism. This incidence angle is known as resonance angle, and the intensity at this angle is the minimum because the maximum energy is used to gain the wave vector matching condition. To regain this wave vector matching condition, one has to change the incidence angle. This change in the incidence angle is measured corresponding to the change in either thickness or refractive index or extinction coefficient. And after proper scaling, one can measure the change in thickness, refractive index, and extinction coefficient by measuring the change in the resonance angle.

2.2 Mathematical concept for reflectivity

At the metal-dielectric interface, the coupling of incident light with the SPs wave is given as

$$\frac{2\pi}{\lambda} n_{\text{prism}} \sin\theta_{\text{SPR}} = \text{real}\left(\frac{2\pi}{\lambda} \sqrt{\frac{\varepsilon_g \varepsilon_s}{\varepsilon_g + \varepsilon_s}} \right) \tag{1}$$

where ε_g and ε_s are dielectric constants of the metallayer (gold) and sensing layer, respectively, and n_{prism} is the refractive index of the prism. The angle of the minimum reflectance is called as the resonance angle or SPR angle (θ_{SPR}), at this point, SPR curve dip is obtained. This SPR curve dip changes by changing the RI of the sensing layer.

Let's take a generalized *N*-layer model to produce an SPR curve for the configuration of the SPR sensor as shown in Fig. 1. For calculating the reflectivity of the reflected light of the *N*-layer model, the transfer matrix method is applied. This method is efficient, and no approximations are considered. The first boundary tangential fields are related to the final boundary by the relation as [18]

$$\begin{bmatrix} X_1 \\ Y_1 \end{bmatrix} = A_2 A_3 A_4 A_5 \cdots A_{N-1} \begin{bmatrix} X_{N-1} \\ Y_{N-1} \end{bmatrix} = \mathbf{A} \begin{bmatrix} X_{N-1} \\ Y_{N-1} \end{bmatrix} \tag{2}$$

where X_1 and Y_1 represent the tangential components of electric and magnetic fields respectively at the boundary of the first layer, and X_{N-1} and Y_{N-1} are the corresponding fields at the *N*th layer. For *P* polarized light, the characteristic matrix of the combined structure of the sensor is denoted by A_{ij} as

$$A_{ij} = \left(\prod_{q-2}^{N-1} A_k \right)_{ij} = \begin{bmatrix} A_{11} A_{12} \\ A_{21} A_{22} \end{bmatrix} \tag{3}$$

$$\text{with} \quad A_k = \begin{bmatrix} \cos\beta_k & -\text{i}\sin(\beta_k / q_k) \\ -\text{i} q_k \sin\beta_k & \cos\beta_k \end{bmatrix} \tag{4}$$

where $q_k = (\mu_k / \varepsilon_k)^{1/2} \cos\theta_k$, and $\beta_k = \dfrac{2\pi}{\lambda} n_k \cos\theta_k (d_k)$.

One can get the value of the reflection coefficient for p polarized light by driving some mathematical steps as follows:

$$r_p = \frac{(A_{11} + A_{12} q_n) q_1 - (A_{21} + A_{22} q_n)}{(A_{11} + A_{12} q_n) q_1 + (A_{21} + A_{22} q_n)}. \tag{5}$$

Finally, the reflectivity *R* of the given multilayer structure is directly related to the reflection coefficient as follows:

$$R = | r_p |^2 . \tag{6}$$

2.3 Performance parameter

The sensitivity (S) of the proposed SPR sensor is computed as the ratio of change in the SPR resonance angle $\delta\theta_{\text{SPR}}$ to minute change in the refractive index of sensing medium (δn_s). Therefore, the sensitivity (degree/RIU) is given as $S = \dfrac{\delta\theta_{\text{SPR}}}{\delta n_s}$ [8]. Actually, the total sensitivity (S_{total}) of the surface plasmon resonance depends on both the change in the refractive index and molecular interaction behavior of the sensing medium on the top layered nanomaterial. Hence, the complete definition can be given as

$$S_{\text{total}} = S \cdot E \tag{7}$$

where E represents the absorption efficiency of the antigen or antibody. In this paper, only S is targeted to observe. Detection accuracy (D.A.) is given by $\dfrac{\delta\theta_{\text{SPR}}}{\delta\theta_{0.5}}$, where $\delta\theta_{0.5}$ is the full width at half maxima ($\delta_{0.5}$) of reflectance curve. D.A. is a unitless parameter. Quality factor (RIU^{-1}) depends upon $\delta_{0.5}$ and sensitivity. It is given by $Q = \dfrac{S}{\delta\theta_{0.5}}$ [9].

3. Results and discussion

The aim is to see the effect of the absorbance of biomolecules on the sensing surface. The reflectance curves for structure-I, i.e., the proposed SPR sensor, structure-II, i.e., the SPR sensor without silicon, and structure-III, i.e., the conventional SPR sensor before and after the adsorption of biomolecules, are shown in Fig. 2. It can be said that as the RI of sensing layer changes from that of pure water to that of impure water (1.33 to 1.36), the reflectance dip change towards a higher value of θ_{SPR}. Figure 2 depicts the change in $\delta\theta_{\text{SPR}}$ before and after the adsorption of the analyte. In Fig. 2, $\delta\theta_{\text{SPR}}$ is 6.92°, 4.78°, and 4.52° for structure-I, structure-II, and structure-III, respectively. This shift in the resonance angle is summarized for structure-I to structure-III in Table 2. It is observed that structure-I has the highest change in the resonance angle which results in a higher sensitivity. Further, the quality factor and detection accuracy are also analyzed. It is also seen that the inclusion of blue P/MoS_2 hetero-structure and silicon layer increases the value of $\delta_{0.5}$ due to the damping of the surface plasmon [8, 10, 16]. In structure-I, the detection accuracy and quality factor are slightly decreased compared with those of structure-II and structure-III. The obtained results are arranged in Table 3.

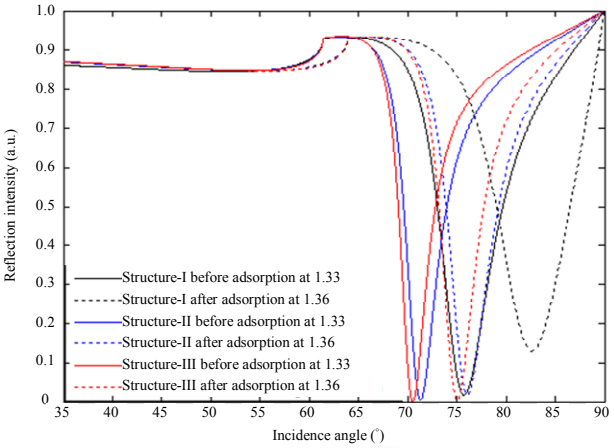

Fig. 2 Reflectance curves for structure-I, structure-II, and structure-III, at the operating wavelength 632.8 nm before and after the adsorption of biomolecules on the sensor surface.

From Table 3, It is observed that the maximum sensitivity is obtained for the proposed sensor structure i.e., structure-I with the moderate detection accuracy and quality factor.

Figure 3 indicates the variation in sensitivity with increasing RI of the sensing layer for all the SPR sensor structures. For structure-I, the sensitivity increases with an increase in the RI from 60°/RIU at RI of pure water to 291°/RIU RI of impure water, for structure-II from 45.33°/RIU to 204.66°/RIU and for structure-III from 43.33°/RIU to 194°/RIU. In this figure, the sensitivity is enhanced for the proposed sensor, i.e., structure-I in comparison with structure-II and structure-III. Since the extinction coefficient is responsible for the absorption of the wave in structure-I due to the blue P/MoS_2 layer. Thus, it disturbs the wave vector matching condition more with respect to other two structures. Structure-I

has a larger shift in the resonance angle because the evanescent field maximizes into the sensing layer by an introduction of blue P/MoS_2 hetero-structure and silicon layer. Sensing layer's refractive index modifies the propagating conditions for the evanescent field which in turn produces a significant change in propagation waves of SPs leading to a larger resonance angle shift [9]. However, for structure-II i.e., blue P/MoS_2 hetero-structure without the silicon layer, an increase in the sensitivity is less compared with that of structure-I.

Table 2 Comparison table for the change in the resonance angle for structure-I, structure-II, and structure-III.

Structure-I			Structure-II			Structure-III		
Resonance angle of pure water (before adsorption)	Resonance angle of impure water (after adsorption)	Shift in resonance angle ($\delta\theta_{SPR}$)	Resonance angle of pure water (before adsorption)	Resonance angle of impure water (after adsorption)	Shift in resonance angle ($\delta\theta_{SPR}$)	Resonance angle of pure water (before adsorption)	Resonance angle of impure water (after adsorption)	Shift in resonance angle ($\delta\theta_{SPR}$)
75.74	82.66	6.92	71.31	76.09	4.78	70.52	75.04	4.52

Table 3 Comparison table for sensitivity, detection accuracy, and quality factor.

Sensor structure	Sensitivity (°/RIU)	Detection accuracy	Quality factor (RIU^{-1})
Structure-I	230.66	1.04	34.58
Structure-II	159.33	1.08	36.29
Structure-III	150.66	1.19	39.75

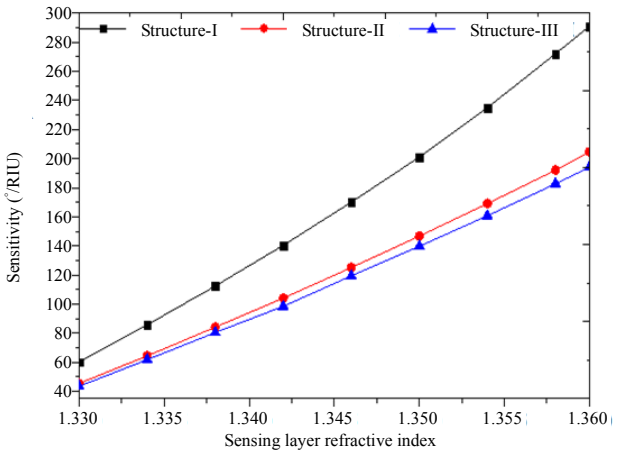

Fig. 3 Variation of sensitivity as a function of the sensing layer' refractive indices for structure-I, structure-II, and structure-III.

Figures 4 and 5 depict the variations in detection accuracy and quality factor with the sensing layer RI for structure-I, structure-II, and structure-III, respectively. It can be observed from Fig. 4 that the detection accuracy increases with sensing layer RI for all three structures. It is also seen that structure-I shows a lower detection accuracy due to the broader reflectance curve or higher value of $\delta_{0.5}$. The broadness in the reflectance curve is due to plasmon damping, and this similar behavior has already been reported by Pockrand *et al.* [19]. Therefore, the addition of blue P/MoS_2 hetero-structure and silicon layer enhances the sensitivity as shown in Fig. 3, however, at the same time, it broadens the reflectance curve. Therefore, blue P/MoS_2 hetero-structure and silicon layer affect the detection accuracy as shown in Fig. 4. It can be observed from Fig. 5 that the quality factor increases with an increase in RI of the sensing layer for all three structures.

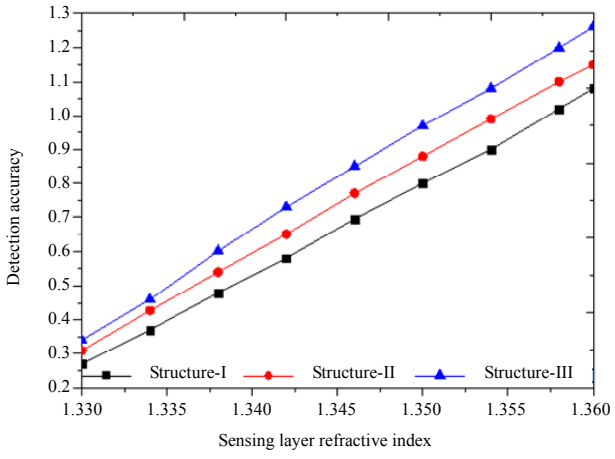

Fig. 4 Variation of the detection accuracy as a function of the sensing layer refractive index for structure-I, structure-II, and structure-III.

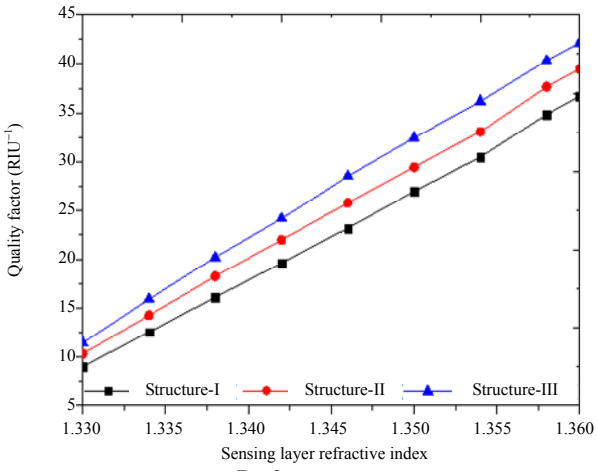

Fig. 5 Variation of the quality factor as a function of the sensing layer' refractive indices for structure-I, structure-II, and structure-III.

It is also observed that blue P/MoS_2 hetero-structure and silicon layer-based sensor i.e., structure-I lead to a reduced quality factor because the quality factor is a linear inverse function of $\delta_{0.5}$, so the maximum $\delta_{0.5}$ indicates a lower quality factor. The observation of the effect of the silicon layer thickness on the proposed SPR sensor, i.e., structure-I, is summarized in Table 4. At a fixed wavelength, it is observed that the sensitivity increases with an increase in the silicon layer thickness up to 2.5 nm while the detection accuracy and quality factor decreases for the proposed sensor, i.e., structure-I. Therefore, a silicon layer thickness of 2.0 nm is used because, at this thickness, the quality factor and detection accuracy are moderate with the high sensitivity.

Table 4 Effect of the silicon layer thickness at the operating wavelength 632.8 nm on the sensitivity, detection accuracy, and quality factor of the proposed SPR sensor, i.e., structure-I.

Thickness of silicon layer (nm)	Sensitivity (°/RIU)	Detection accuracy	Quality factor (RIU^{-1})
0.0	159.33	1.08	36.29
1.0	185.33	1.03	34.44
1.5	205.00	1.02	34.28
2.0	230.66	1.04	34.58
2.5	247.66	1.00	33.42
3.0	153.00	0.56	18.72

In Fig. 6(a), the surface plasmon resonance curves are plotted for various numbers of layers of blue P/MoS_2 heterostructure (L) at the thickness of the silicon layer at 2.5 nm. It is seen from Fig. 6(a) that the surface plasmon resonance curves become shallower and broader as L increases from 1 to 10. This is just because of the non-zero extinction coefficient of blue P/MoS_2 hetero-structure which is responsible for reducing the propagation velocity of the electromagnetic wave in it with respect to sensing medium [19]. This decrement in the velocity is responsible for the damping of surface plasmon in the blue P/MoS_2 hetero-structure [19]. On increasing the number of layers of blue P/MoS_2 hetero-structure, the thickness and effective extinction coefficient increase, as a result, the damping of surface plasmons enhances. Due to the damping of surface plasmons, resonance curves become broader and shallower. The broadening and shallowing of the resonance curve increases with the number of blue P/MoS_2 hetero-structure which can be clearly observed from Fig. 6(a). Further, the sensitivity, detection accuracy, and quality factors are calculated corresponding to the resonance curves in Fig. 6(a) and plotted in Fig. 6(b) for L = 1 to L = 6 at the thickness of the silicon layer at 2.5 nm. It can be observed from Fig. 6(b) that the sensitivity is the highest for the bilayer blue P/MoS_2 hetero-structure but the detection accuracy and quality factor decrease with respect to monolayer. Beyond L = 2, the performance of the sensor decreases in all respect, i.e., the sensitivity, detection accuracy, and quality factor. One can observe from Fig. 6(a) that beyond L = 6, the SPR dip is very broad because of increased damping, due to which the minimum reflection intensity could not be calculated exactly. Hence, the results in Fig. 6(b) beyond L = 6 are not useful at all. Hence, it can be said that the monolayer blue P/MoS_2 hetero-structure has the best performance. One can choose bilayer blue P/MoS_2 hetero-structure, but with reduced detection

accuracy and quality factor. Transverse magnetic (TM) field intensity is obtained for structure-I, structure-II, and structure-III by using the transfer matrix method, which is shown in Figs. 7(a) to 7(c). It is clear from Fig. 7 that field distributions are in the expected shape.

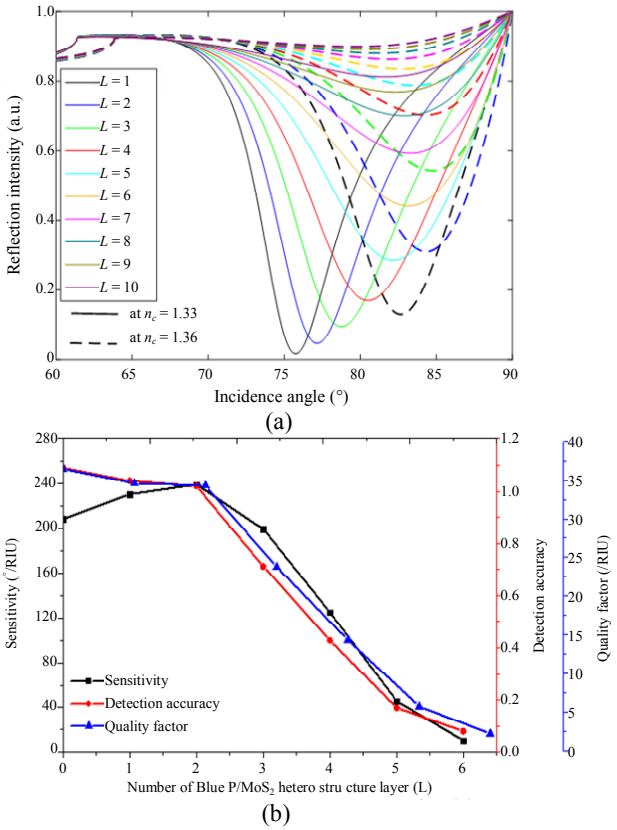

Fig. 6 Effect of increasing the number of blue P/MoS_2 hetero-structure layer on: (a) surface plasmon resonance curve and (b) sensitivity, detection accuracy, and quality factor.

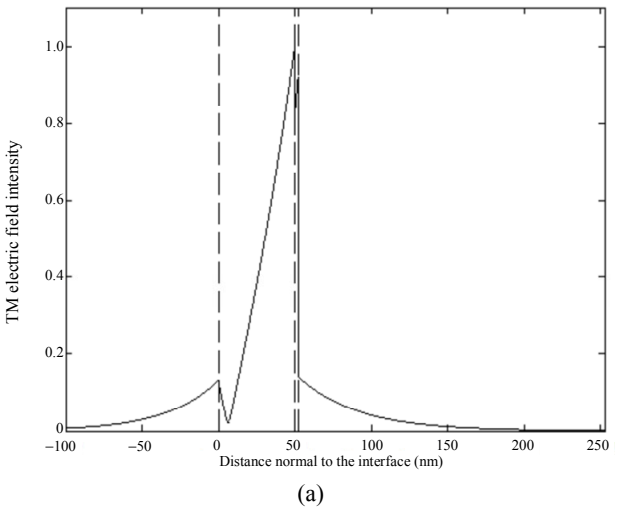

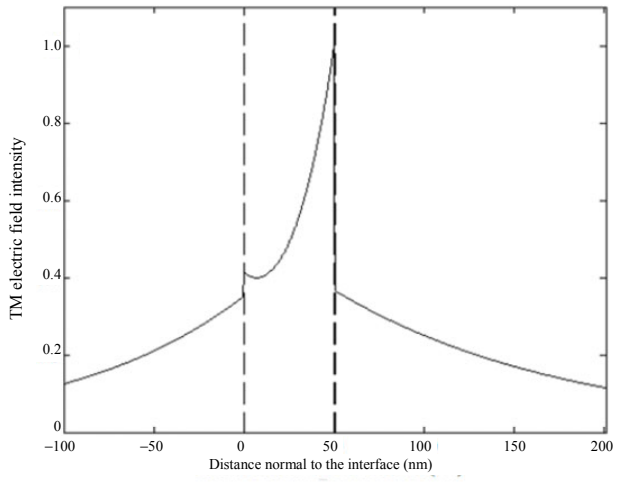

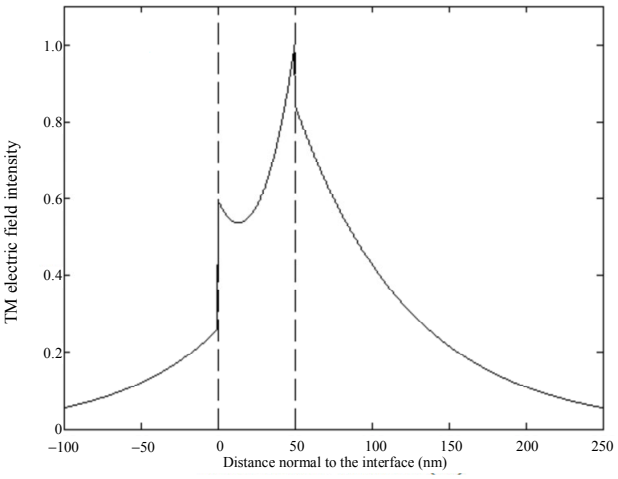

Fig. 7 TM field intensity as a function of distance normal to the interface at the sensing layer refractive index of 1.33, for the SPR sensors based: (a) structure-I, (b) structure-II, and (c) structure-III.

4. Conclusions

The proposed blue P/MoS_2 hetero-structure based SPR sensor confirms a fairly good performance parameter, compared with a conventional SPR sensor. It is found that a significant increase in the sensitivity from 150.66 °/RIU to 230.66 °/RIU is observed in comparison with the conventional SPR sensor after utilizing blue P/MoS_2 hetero-structure. Further, an additional silicon nanolayer of thickness 2.0 nm is used between the metal layer and blue P/MoS_2, and

a significant increase in the sensitivity with a moderate quality factor and detection accuracy is observed. It concludes that the thickness of the siliconlayer plays a vital role in SPR sensor performance, and it is found that 2 nm thickness is best suited for the good performance of the proposed SPR sensor. Therefore, the proposed sensor could find potential applications in the area of biosensing and gas sensing.

Acknowledgement

This work is partially supported under Project No. 34/14/10/2017-BRNS/34285 by Board of Research in Nuclear Sciences (BRNS), Department of Atomic Energy (DAE), Government of India.

References

[1] C. T. Li, H. F. Chen, I. W. Un, H. C. Lee, and T. J. Yen, "Study of optical phase transduction on localized surface plasmon resonance for ultrasensitive detection," *Optics Express*, 2012, 20(3): 3250–3260.

[2] J. Hamola, S. S. Yee, and G. Gauglitzand, "Surface plasmon resonance sensor: review," *Analytical Sensors Actuators B*, 1999, 54(1–2): 3–15.

[3] S. Pal, Y. K. Prajapati, J. P. Saini, and V. Singh, "Resolution enhancement of optical SPR sensor using metamaterial," *Photonic Sensors*, 2015, 5(4): 330–338.

[4] F. S. Ligler, C. R. Taitt, L. C. S. Lake, K. E. Sapsford, Y. Shubin, and J. P. Golden, "Array bio-sensors for detection of toxins," *Analytical and Bioanalytical Chemistry*, 2003, 377(3): 469–477.

[5] L. M. Wu, Y. Jia, L. Y. Jiang, J. Guo, X. Y. Dai, Y. J. Xiang, *et al.*, "Sensitivity improved SPR biosensor based on the MoS_2/Graphene–Aluminum hybrid structure," *Journal of Lightwave Technology*, 2017, 35(1): 82–87.

[6] J. B. Maurya and Y. K. Prajapati, "A comparative study of different metal and prism in the surface plasmon resonance biosensor having MoS_2-Graphene," *Optical and Quantum Electronics*, 2016, 48(5): 280-1–280-12.

[7] J. B. Maurya, A. François, and Y. K. Prajapati, "Two-dimensional layered nanomaterial based one-dimensional photonic crystal refractive index sensor," *Sensors*, 2018, 18(3): 857-1–857-7.

[8] S. Pal, A. Verma, Y. K. Prajapati, and J. P. Saini, "Influence of black phosphorous on performance of surface plasmon resonance biosensor," *Optical and Quantum Electronics*, 2017, 49: 403-1–403-13.

[9] S. Pal, A. Verma, S. Raikwar, Y. K. Prajapati, and J. P. Saini, "Detection of DNA hybridization using black phosphorus-graphene coated surface plasmon resonance sensor," *Applied Physics A*, 2018, 124(5): 394-1–394-11.

[10] J. B. Maurya, S. Raikawar, Y. K. Prajapati, and J. P. Saini, "A silicon-black phosphorous based surface plasmon resonance sensor for the detection of NO_2 gas," *Optik*, 2018, 160: 428–433.

[11] J. B. Maurya, Y. K. Prajapati, V. Singh, and J. P. Saini, "Sensitivity enhancement of surface plasmon resonance sensor based on graphene-MoS_2 hybrid structure with TiO_2-SiO_2 composite layer," *Applied Physics A*, 2015, 121(2): 525–533.

[12] Q. L. Ouyang, S. W. Zeng, J. Li, L. Y. Hong, G. X. Xu, X. Q. Dinh, *et al.*, "Sensitivity enhancement of transition metal dichalcogenides/silicon nanostructure-based surface plasmon resonance biosensor," *Scientific Reports*, 2016, 6: 28190-1–28190-13.

[13] L. M. Wu, J. Guo, Q. K. Wang, S. B. Lu, X. Y. Dai, Y. J. Xiang, *et al.*, "Sensitivity enhancement by using few-layer black phosphorus-graphene/TMDCs heterostructure in surface plasmon resonance biochemical sensor," *Sensors and Actuators B: Chemical*, 2017, 249: 542–548.

[14] S. M. Cui, H. H. Pu, S. A. Wells, Z. H. Wen, S. Mao, J. B. Chang, *et al.*, "Ultrahigh sensitivity and layer-dependent sensing performance of phosphorene-based gas sensors," *Nature Communications*, 2015, 6: 8632-1–8632-9.

[15] N. S. Liu and S. Zhou, "Gas adsorption on monolayer blue phosphorus: implications for environmental stability and gas sensors," *Nanotechnology*, 2017, 28(17): 175708-1–175708-9.

[16] Q. Peng, Z. Y. Wang, B. S. Sa, B. Wu, and Z. M. Sun, "Electronic structures and enhanced optical properties of blue phosphorene/transition metal dichalcogenides van der Waals heterostructures," *Scientific Reports*, 2016, 6: 31994-1–

31994-10.
[17] A. Lahav, M. Auslender, and I. Abdulhalim, "Sensitivity enhancement of the guided wave surface-plasmon resonance sensors," *Optics Letters*, 2008, 33(21): 2539–2541.
[18] J. B. Maurya, Y. K. Prajapati, V. Singh, J. P. Saini, and R. Tripathi, "Performance of graphene-MoS_2 based surface plasmon resonance sensor using silicon layer," *Optical and Quantum Electronics*, 2015, 47(11): 3599–3611.
[19] I. Pockrand, J. D. Swalen, J. G. Gordon, and M. R. Phllpott, "Surface plasmon spectroscopy of organic monolayer assemblies," *Surface Science*, 1977, 74: 237–244.